Reaction Mechanism and Structure – Reactivity Relationships in the Stereospecific 1,4-Polymerization of Butadiene Catalyzed by Neutral Dimeric Allylnickel(II) Halides $[Ni(C_3H_5)X]_2$ ($X^- = Cl^-$, Br^-, I^-): A Comprehensive Density Functional Theory Study

Sven Tobisch*[a] and Rudolf Taube[b]

Abstract: For the first time, a comprehensive and consistent picture of the catalytic cycle of 1,4-polymerization of butadiene with neutral dimeric allylnickel(II) halides $[Ni(C_3H_5)X]_2$ ($X^- = Cl^-$ (**I**), Br^- (**II**), and I^- (**III**)) as single-site catalysts has been derived by means of quantum chemical calculations that employ a gradient-corrected density-functional method. All crucial reaction steps of the entire catalytic course have been scrutinized, taking into account butadiene π complex formation, symmetrical and asymmetrical splitting of dimeric π complexes, *cis*-butadiene insertion, and *anti* – *syn* isomerization. The present investigation examines, in terms of located structures, energies and activation barriers, the participation of postulated intermediates, in particular it aimed to clarify whether monomeric or dimeric species are the catalytically active species. Prior qualitative mechanistic assumptions are substituted by the presented theoretically well-founded and detailed analysis of both the thermodynamic and the kinetic aspects, that substantially improve the insight into the reaction course and enlarge them with novel mechanistic proposals. From a mechanistic point of view, all three catalysts exhibit common characteristics. First, chain propagation occurs by *cis*-butadiene insertion into the π-butenylnickel(II) bond with nearly identical intrinsic free-energy activation barriers. Second, the reactivity of *syn*-butenyl forms is distinctly higher than that of *anti* forms. Third, the chain-propagation step is rate-determining in the entire polymerization process, and the preestablished *anti* – *syn* equilibrium can always be regarded as attained. Accordingly, neutral dimeric allylnickel(II) halides catalyze the formation of a stereoregular *trans*-1,4-polymer under kinetic control following the k_{1t} channel with butenyl(halide)(butadiene)Ni^{II} complexes being the catalytically active species. Production of a stereoregular *cis*-1,4-polymer with allylnickel chloride can only be explained by making the k_{2c} channel accessible by the formation of polybutadienyl(butadiene) complexes, which is accompanied by the coordination of the next double bond in the growing chain to the Ni^{II} center.

Keywords: allyl complexes · density functional calculations · nickel · polymerization · reaction mechanisms · structure – reactivity relationships

Introduction

The transition metal catalyzed polymerization of butadiene is a scientifically as well as a technically important process.[1, 2] From a mechanistic point of view, the diene polymerization, as a chemo-, regio-, and stereoselective C–C bond formation reaction is of fundamental importance. Conjugated diene polymerization is an insertion polymerization,[3] as is that of the monoalkene. It is generally accepted that chain propagation proceeds in two steps: by coordination of free monomer and subsequent insertion into the transition metal carbon bond of the terminal group on the reactive growing chain. There are two important differences between the polymerization of 1-alkenes of 1,3-dienes.

First, the transition metal carbon bond is of the σ-type for 1-alkenes and of the allylic π-type for 1,3-dienes. The allyl-insertion mechanism has been proven by ^1H and ^{13}C NMR spectroscopy for both *trans*-regulating (e.g. $[Ni(C_4H_7)I]_2$[4]) and *cis*-regulating (e.g. $[Ni(C_3H_5)O_2CCF_3]_2$[5]) butadiene-polymerization catalysts. The transition metal butenyl π bond has peculiar features which are responsible for the particular characteristics of diene polymerization. The bond between the η^3-butenyl group and the transition metal can exist in two isomeric forms, namely *anti* and *syn*, which are in equilibrium.

[a] Dr. S. Tobisch
Institut für Anorganische Chemie der Martin-Luther-Universität Halle-Wittenberg Fachbereich Chemie, Kurt-Mothes-Strasse 2
06210 Halle (Germany)
Fax: (+49) 345-5527028
E-mail: tobisch@chemie.uni-halle.de

[b] Prof. Dr. R. Taube
Fuchsienweg 17
06118 Halle (Germany)

Supporting information for this article is available on the WWW under http://www.wiley-vch.de/home/chemistry or from the author.

  0947-6539/01/0717-3681 $ 17.50+.50/0

According to the generally accepted *anti–cis* and *syn–trans* correlation, butadiene insertion gives rise to a *cis* or a *trans* double bond in the newly formed C_4 unit of the growing polymer chain, when starting from an *anti*- or *syn*-butenyl group. Another characteristic of the transition metal butenyl bond is that it has two reactive sites, C^1 and C^3, which for example, may give rise to 1,4- and 1,2-polymers.

Second, 1,3-dienes have a greater diversity than 1-alkenes in their coordination to a transition metal. 1,3-Diene coordination can occur in two different modes: monodentate (η^2) or bidentate (η^4), either from the s-*trans* or the s-*cis* configuration. An *anti*- or *syn*-butenyl terminal group is formed under kinetic control by diene insertion to occur from the s-*cis* or s-*trans* configuration, respectively. The mechanism of stereoregulation of 1,3-diene polymerization, which to date has not been completely understood[1] is, therefore, much more complicated than the polymerization of 1-alkenes.

For a basic understanding of the *cis–trans* regulation of diene polymerization, two different processes must be interrelated, namely the *anti–syn* isomerization and the monomer-insertion processes. For the chain-propagation step, two commonly accepted mechanisms were proposed which differ with regard to the suggested insertion mode of the butenyl group. On the one hand, the σ-allyl insertion mechanism, suggested by Cossee and Arlman,[6] in which the butenyl group in η^1-σ coordination should react like an alkyl group. In contrast, Taube et al.[7] suggested that the C–C bond formation can also proceed through a nucleophilic attack of the η^3-π-butenyl group on the diene.

In a series of papers,[8] we have applied density functional theory to shed light on the mechanistic aspects of the stereospecific polymerization of butadiene. We have focused on the π-allyl-insertion mechanism, which is explored with experimentally well-characterized catalysts for the Ni^{II}-catalyzed stereospecific butadiene polymerization, as an example. In the first step, we demonstrated that butadiene insertion into the butenylnickel(II) bond is energetically feasible within the π-coordination of both reacting moieties.[8a] We were able to deduce structure–activity relationships, which are responsible for opening that reaction channel which yields *trans*-1,4 and *cis*-1,4 polymer units, respectively, by a theoretical examination of the entire polymer-generation cycle for typical *trans*-regulating catalysts, that is, cationic and neutral butenyl(monoligand)(butadiene)nickel(II) complexes,[8b] and *cis*-regulating catalysts, that is, cationic polybutadienyl(butadiene)nickel(II) complexes.[8c]

In the present study, the stereoregulation mechanism is theoretically explored for the 1,4-polymerization of butadiene mediated by neutral dimeric allylnickel(II) halides $[Ni(C_3H_5)X]_2$ where $X^- = Cl^-$ (**I**), Br^- (**II**), and I^- (**III**). The dimeric allylnickel(II) halides have been discovered as the first one-component butadiene polymerization catalysts.[4, 9–11] All of them catalyze the C^1–C^1 bond formation, which yields almost exclusively 1,4-polymers. Compound **III** gives a polymer of predominantly *trans*-1,4 structure, **I** gives a polymer of predominantly *cis*-1,4 structure, whilst **II** gives a statistical *cis*/*trans* equibinary polybutadiene that consists of approximately 50% *cis* and 50% *trans* polymer units.[9b, 10a, 10d] Under comparable conditions, experiments verified the catalytic activity of **III** as moderate, of **II** as low, and **I** as only very weak.[10d, 11a,b] The dimeric allylnickel(II) halides, at least the iodide, are probably the most extensive experimentally investigated diene-polymerization catalyst systems. While much understanding of the catalytic cycle has been achieved, mechanistic details still remain unclarified. For example, which factors determine the different catalytic activity and stereoselectivity observed for the three catalysts? How does the equilibrium between dimeric and monomeric catalyst complexes influence the entire polymerization reaction? Computational chemistry might give an answer to these and related intriguing questions by providing a detailed picture of the catalytic cycle including both kinetic and thermodynamic aspects. To the best of our knowledge, a theoretical mechanistic study on the title reaction has not yet been reported. Herein, we present a comprehensive and well-founded view of the entire polymer-generating cycle with the aim to make a contribution to enlighten the mechanism of stereoregulation.

The known mechanistic details for the butadiene polymerization mediated by allylnickel(II) halides can be summarized as follows: 1) NMR investigation conclusively established for the iodide, that chain propagation occurs by means of *cis*-butadiene insertion.[10g–i] An *anti*-butenyl group is regenerated as the end of the reactive growing chain in the kinetic insertion products, which subsequently undergoes *anti–syn* isomerization to give the thermodynamically more stable *syn*-butenyl form. 2) Experiment showed, for iodide, that butadiene insertion is a relatively slow process. Isomerization could not be observed by NMR spectroscopy under polymerization conditions, presumably because this process is too fast. In the reaction solution with butadiene, only the *syn*-butenyl form could be detected.[9f, 10e,h] As a result of the *anti* insertion, one must conclude that isomerization is much more rapid than insertion. The thermodynamically more stable *syn*-butenyl form must also be more reactive than the *anti*-butenyl counterpart, since a polymer of predominantly *trans*-1,4 structure is generated with the iodide. In the case of the iodide-catalyzed 2-alkylbutadiene polymerization, the rate of isomerization was found to be two orders of magnitude greater than the insertion rate.[10i] The isomerization rate, however, was determined at the end of the polymerization reaction after all the diene had been consumed. An acceleration of the isomerization can be expected in the presence of monomers. Overall, for iodide, experiment clearly indicates that isomerization is much more rapid than insertion and therefore *cis*-butadiene insertion should be the rate-determining step. 3) Kinetic studies showed, for the iodide[9c, 11a,b] as well as for the bromide and the chloride,[11a,b] that the overall rate of the polymerization process is first-order in monomer and half-order in catalyst concentration according to the rate law $r_p = k_p[Ni_2]^{0.5}[C_4H_6]$.[9c, 11a,b] A dissociative equilibrium between dimeric and monomeric butadiene π complexes must be assumed according to Equations (1), (2), and (3), where C_2X_2 = catalyst dimer and M = monomer.

$$C_2X_2 + M \rightleftharpoons C_2X_2(M) \quad (1)$$

$$C_2X_2(M) + M \rightleftharpoons C_2X_2(M)_2 \quad (2)$$

$$C_2X_2(M)_2 \rightleftharpoons 2\,CX(M) \quad (3)$$

0947-6539/01/0717-3682 $ 17.50+.50/0 *Chem. Eur. J.* **2001**, *7*, No. 17

From the half-order dependence on the catalyst concentration it was concluded that the dimeric forms are inactive and chain propagation occurs via monomeric complexes.[9b,c, 11a] For iodine, a different dependence of the overall rate on the monomer and catalyst concentrations was observed when an expanded concentration range was investigated. At high monomer concentrations, the rate was found to be half-order in monomer.[9d] At very low[11c] or very high[10f] catalyst concentrations, a first-order dependence on the catalyst concentration was observed. Kormer et al.[10f,i] concluded that dimeric π complexes are also active species capable of achieving insertion: this is verified for iodide-catalyzed polymerization of 2-alkylbutadienes. 4) Whether isomerization does indeed occur via the dimeric or monomeric species is not known.

Computational Model and Method

Models: Geometries and relative energies of the reactants, intermediates, transition states, and products of competitive chain-propagation cycles as well as of *anti–syn* isomerization reactions were calculated with a gradient-corrected density-functional method, which has been shown to be quite reliable both in geometry and in energy. To keep the computational effort moderate, the butenyl group, which includes the noncoordinating growing polymer chain was mimicked by a crotyl group; $R = CH_3$ was adopted for the butadiene π complexes that formed under polymerization conditions $[RC_3H_4Ni(C_4H_6)X]$ with $X^- = Cl^-$, Br^-, I^- for monomeric and $X^- = [RC_3H_4NiY_2]^-$, $Y^- = Cl^-$, Br^-, I^- for dimeric complexes. Dimeric bis-butadiene π complexes of the general formula $C_2X_2(M)_2$ (cf. Equations (2) and (3)) were not explicitly considered since they represent highly unstable intermediates whose thermodynamic population must be regarded as very small (see below). The optimized geometries of key structures of the polymerization cycle, given below, were restricted to the case of the chloride.

Our investigations focus on the polymerization cycle and the initialization step; the formation of the dimeric butenylnickel(II) halides from the allylnickel(II) halide starting material, will not be considered. We restricted our examination to the *cis*-butadiene insertion, and did not take into consideration the alternative insertion of butadiene from its s-*trans* configuration. A justification for neglecting this reaction pathway has been given in the case of nickel, both by experimental[7a, 10g–i, 12] and theoretical[8b] evidence, which convincingly establish the *anti*-insertion process. The effect of the solvent on the catalytic cycle was neglected since there is no experimental evidence that the catalytic activity or *cis–trans* selectivity is significantly influenced for polymerization to occur in noncoordinating solvents.

Parts of the catalytic cycle have already been investigated in our previous study.[8b] This research, however, was restricted to the iodide catalyst. The equilibrium between dimeric and monomeric butadiene π complexes have been not taken into account in this study and only precursors of the real isomerization transition states have been reported.

The intrinsic energy of inserting s-*cis*-butadiene into a C–C bond (the energy gain from breaking one C–C double bond and forming a C–C single bond during the insertion) without a catalytically active Ni^{II} center was estimated as the average value of the exothermicities which were obtained for the general reaction given in Equation (4).

$$C_4H_7\text{-}(C_4H_6)_n\text{-}C_4H_7 + C_4H_6 \longrightarrow C_4H_7\text{-}(C_4H_6)_{n+1}\text{-}C_4H_7 \ (n = 0-2) \qquad (4)$$

This amounts to 20.3 (ΔE) and 17.4 kcal mol^{-1} (ΔH). A value of 18.7 kcal mol^{-1} was obtained experimentally for polymerization occurring in the gas phase.[13]

Method: All reported calculations were performed with the DGauss program within the UniChem software environment[14] and the program package TURBOMOLE,[15] developed by Ahlrichs et al. at the University of Karlsruhe (Germany). The calculations were carried out by the use of LDA with Slater's exchange functional[16a,b] and Vosko–Wilk–Nusair parameterization on the homogeneous electron gas for correlation,[16c] augmented by gradient corrections to the exchange-correlation potential. Gradient corrections for exchange based on the functional of Becke[16d] and for correlation based on Perdew[16e] were added variationally within the SCF procedure (BP86).

All-electron Gaussian-orbital basis sets were used for all atoms except for the halides. The geometry optimization, the saddle-point search, and the frequency calculations were performed with a standard DZVP basis set which consists of a 15s/9p/5d set contracted to (63321/531/41) for nickel,[17a] a 9s/5p/1d set contracted to (621/41/1) for carbon,[17b] and a 5s set contracted to (41) for hydrogen.[17b] The energy was evaluated for the optimized structures with the Wachters 14s/9p/5d set[17c] supplemented by two diffuse p[17c] and one diffuse d function[17d] contracted to (62111111/5111111/3111) for nickel, and a TZVP basis for carbon[17b] (a 10s/6p/1d set contracted to (7111/411/1)) and for hydrogen[17b] (a 5s/1p set contracted to (311/1)). For the halides, the Stuttgart ECP's[17e] that replaces all core electrons except for the valence ns^2np^5 electrons and the corresponding 4s/5p/1d set contracted to (31/311/1) were adopted. The corresponding auxiliary basis sets were used to fit the charge density.[17b,f] This is the standard computational methodology utilized throughout this paper.

The geometry optimization and the saddle-point search were carried out at the BP86 level of approximation by the use of analytical gradients/Hessians according to standard algorithms. No symmetry constraints were imposed in any case. The stationary points were identified exactly by the curvature of the potential-energy surface at these points corresponding to the eigenvalues of the analytically calculated Hessian.

The reaction and activation enthalpies (ΔH and $\Delta H^{\neq}$ at 298 *K* and 1 atm) were calculated for the most stable isomers of each of the key species of the entire catalytic reaction. The complete potential-energy profiles (ΔE) are summarized in four Tables which are included in the Supporting Information. For competitive pathways of monomer insertion and *anti–syn* isomerization, the free activation energies ($\Delta G^{\neq}$ at 298 K and 1 atm) were calculated.

Labeling of the molecules: For each of the dimeric and monomeric butadiene π complexes as well as the corresponding insertion transition states, a number of isomers are possible, which have been carefully explored. They originate from the *anti* and *syn* configuration of the butenyl group and are labeled with an **a** and **s**, respectively. Additionally, four different mutual arrangements of the reacting butenyl and butadiene moieties have been taken into account; they originate from the prone and the opposite supine[18] orientation of both parts (thus giving rise to supine/supine (SS), supine/prone (SP), prone/supine (PS), and prone/prone (PP) arrangements). The structurally different modes of *cis*-butadiene coordination at the metal M in the π complexes are illustrated in Figure 1. For 16-

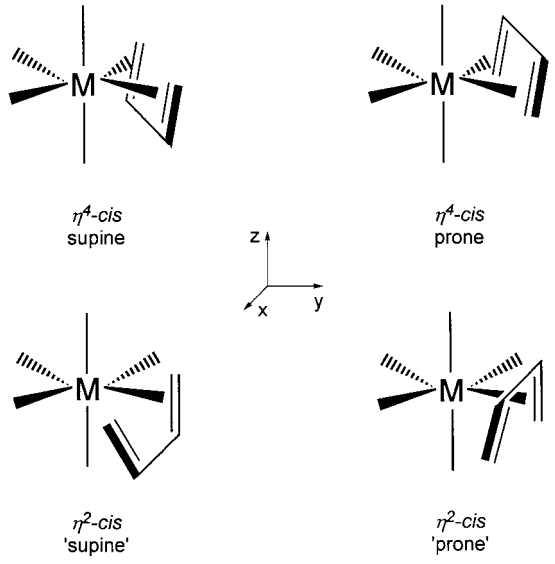

Figure 1. Structurally different modes of *cis*-butadiene coordination at the metal M in butadiene π complexes.

electron square-planar complexes (i.e. monomeric monodentate-coordinated butadiene complexes **3** and insertion products **6**), the SS and PP and the SP and PS orientations are identical with respect to the coordination pattern. To label the different complexes in a consistent manner, the following convention has been adopted throughout this paper. The butenyl and butadiene moieties reside in the square-planar coordination plane (*xy*). Depending on the mode of butadiene coordination, the halides occupy an axial position ($+z$ direction), or a position within the *xy* plane (monomeric complexes), or both of these (dimeric complexes). The orientations of the butenyl and butadiene moieties with the terminal atoms pointing toward or away from the axial ligand have been denoted as supine (S) and prone (P), respectively (cf. Figure 1).

Monomeric complexes will be referred to by a single numeral (**3**, **4**, **5**, **6**, **7**) attached to a lower-case **a** or **s** and two upper-case letters (e.g. **4s**-SS, cf. Scheme 1). The numeric-alphabetic labels have a **2xy** prefix for the corresponding dimeric complexes, where **x** and **y** are related to the *anti*- and *syn*-butenyl forms of both fragments. For dimeric species that contain butadiene, the first letter concerns the fragment in which the butadiene resides (e.g. **2ss-4**SS, cf. Scheme 1).

Results and Discussion

As a result of our calculations, we propose the catalytic cycle given in Scheme 1 for the allylnickel(II) halide catalyzed 1,4-polymerization of butadiene. Dimeric and monomeric butenyl(halide)(butadiene)nickel(II) complexes $[RC_3H_4Ni(C_4H_6)X]$ are supposed to be the catalytically active species. Although they were examined, dimeric insertion transition states are not included for sake of clarity. The thermochemical profile of the entire catalytic cycle is shown in Scheme 1 where the labeling of each species is also given (for the labeling conventions adopted see the Computational Model and Method Section). In Scheme 1, enthalpies for the most stable isomers of each species are given for **I**, **II**, **III**, separated by slashes, with the most stable dimeric bis(butenylnickel halide)(butadiene) complex; namely, **2ss-3**SP, chosen as reference. The intrinsic energy to extend the polymer chain by an additional C_4 unit in subsequent propagation cycles (see the Computational Model and Method Section) is excluded from the energetic profile.

We shall first give an general overview, followed by a discussion of the catalytic cycle step-by-step.

Commencing with the catalyst starting material $[Ni(C_3H_5)X]_2$, dimeric butenylnickel(II) halides C_2X_2, that is $[Ni(RC_3H_4)X]_2$ (**2**), are formed after a short initialization period.[9c] Subsequently, with butadiene dimeric bis(butenylnickel halide)(butadiene) complexes $C_2X_2(M)$ are formed (cf. Equation (1)) which differ with regard to the mode of butadiene coordination, namely, monodentate (or η^2) **2-3**, and bidentate (or η^4) **2-4**. After uptake of a second butadiene and subsequent dissociation, monomeric butenyl(halide)(butadiene)Ni^{II} complexes are formed (cf. reactions in Equations (2) and (3)), in which the coordination of butadiene is either monodentate (**3**) or bidentate (**4**). A rapid dissociative equilibrium can be reasonably supposed between the different π complexes (in accordance with the common experience in Ni^{II} coordination chemistry, with Ni^{II} in a spin-paired d^8 configuration).[19] *cis*-Butadiene insertion can take place in dimeric or monomeric complexes through transition states **2-5** (not included in Scheme 1) or **5**, respectively, which leads to *anti*-butenyl kinetic insertion products in every case. After insertion takes place successfully in monomeric complexes, the polymer chain is elongated by a new C_4 unit that contains one new *cis* (**6a**-*cis*) or *trans* (**6a**-*trans*) double bond, depending on whether the insertion proceeds by k_{1c} or k_{1t}, respectively. The chain propagation continues by replacing the growing chain with uptake of a new butadiene. This results in monomeric π complexes, which may undergo dimerization with the remaining monomeric butadiene complex not involved in the insertion process, thus completing the catalytic cycle. On account of *anti* insertion, the *anti* – *syn* isomerization is a prerequisite step in the polymerization cycle in order to open the route that generates the 1,4-*trans* polymer by k_{1t}. Isomerization can occur in the starting material (indicated by $K_{a/s}{}^{s}$, but not examined in this study) and under polymerization conditions (indicated by $K_{a/s}{}^{p}$), either in dimeric (**2-7**) or in monomeric (**7**) butadiene complexes.

Bis(π-butenylnickel halide) complexes: The optimized geometries of **2** are given in Figure 2 together with relevant structural data. They are calculated to be minima with a square-planar structure that adopt C_2 symmetry for identical butenyl configurations (i.e. **2ss**, **2aa**) and C_1 symmetry for **2sa**. X-ray structures of analogous complexes show that the Ni – halide bond lengths are in the range of 2.24 – 2.25 Å for bis(μ^2-chloro)(1,2,3-η^1-{(trimethylsilyl)oxy-2-butenyl)nickel(II)}[20a] and of 2.33 – 2.38 Å for bis(μ^2-bromo)(2-carboxymethyl)-(π-allyl)nickel(II).[20b] The calculated geometries compare well with the experimental results (see Figure 2 and the Supporting Information).

The *syn*-butenyl forms are calculated to be thermodynamically more stable than their *anti* counterparts. The energetic gap between the isomers is very similar for **I**, **II**, and **III**. **2ss** is the most stable isomer, while **2sa** and **2aa** are separated from it by approximately 1.4 and 2.8 kcal mol^{-1} (ΔH), respectively. The application of Maxwell – Boltzmann statistics (298 K) yields a ratio of 1:11 for **2sa** and 1:110 for **2aa**, with **2ss** in favor. This indicates that the *anti* – *syn* equilibrium in the starting material and in **2** lies in the direction of **2ss** in the absence of butadiene. This agrees with experimental results which indicated that all π-crotylnickel(II) halides are exclusively in the *syn* form.[9e, 10b]

Chain propagation

Formation of butadiene complexes: Monomer π-complex formation is envisioned to proceed in a practically barrierless fashion commencing with **2** by uptake of a single monomer according to Equation (1). Four- and five-coordinate π complexes are expected to be formed in which butadiene preferentially resides in the square-planar (*xy*) coordination plane. Therefore, depending on the mode of butadiene coordination, at least one halide ligand is displaced out of this plane during the process of butadiene uptake.

For butadiene coordination to occur in a monodentate fashion in dimeric complexes, either both halide bridges are retained or one of them is broken. This gives a formal 18-electron five-coordinate square-pyramidal fragment that contains the butadiene in the former case, **2-3**, and a formal 16-electron four-coordinate square-planar fragment in the latter (not shown in Scheme 1). The five-coordinate

0947-6539/01/0717-3684 $ 17.50+.50/0 *Chem. Eur. J.* **2001**, *7*, No. 17

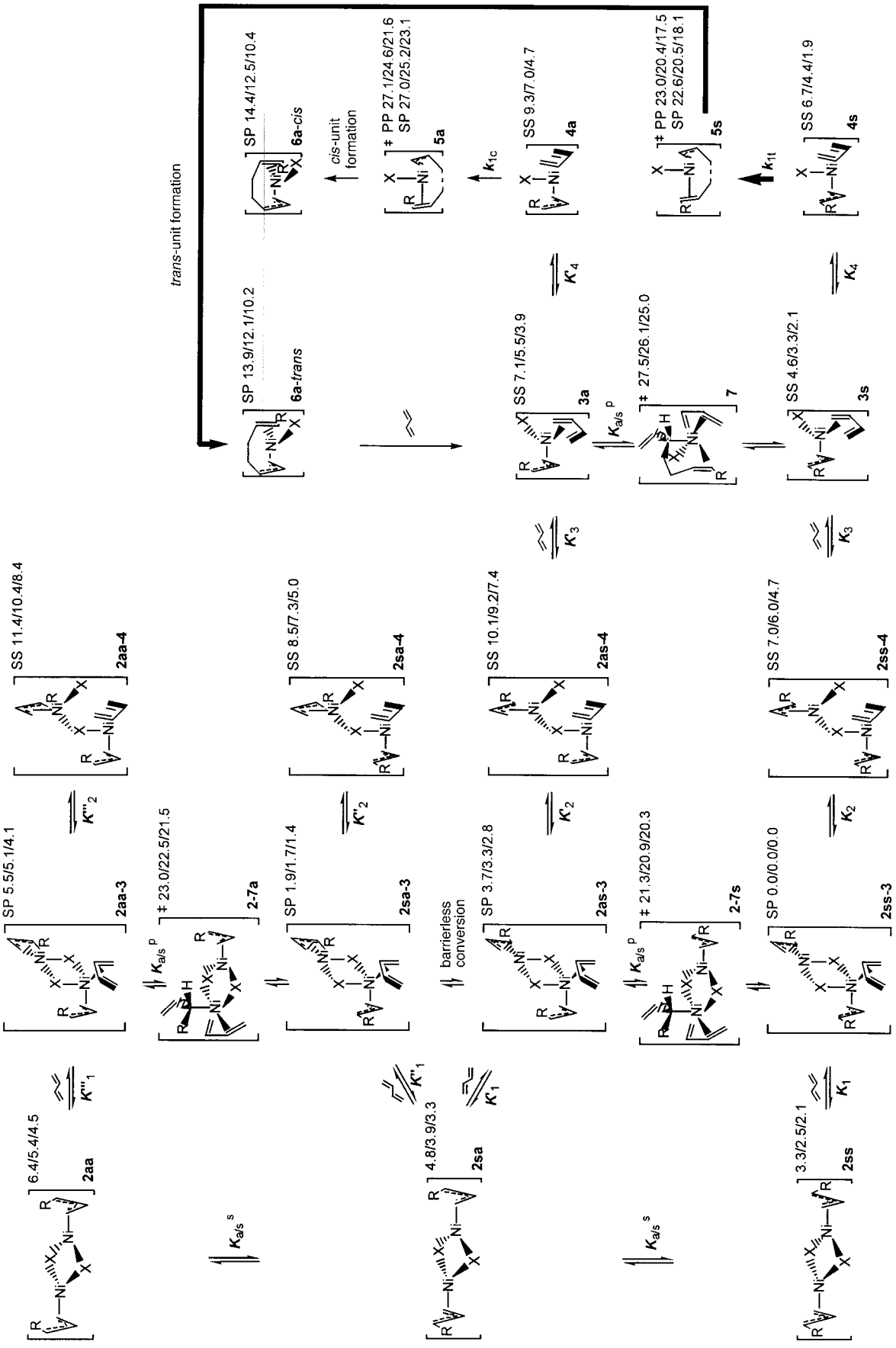

Scheme 1. Thermochemical profile of the proposed catalytic cycle of the 1,4-polymerization of butadiene mediated by neutral dimeric allylnickel(II) halides $[Ni(RC_3H_4)X]_2$ derived from the present study (enthalpies are given in kcal mol^{-1}; see text for details). Dimeric and monomeric butenyl(halide)(butadiene)Ni^{II} complexes $[RC_3H_4Ni(C_4H_6)X]$ are assumed to be the catalytically active species.

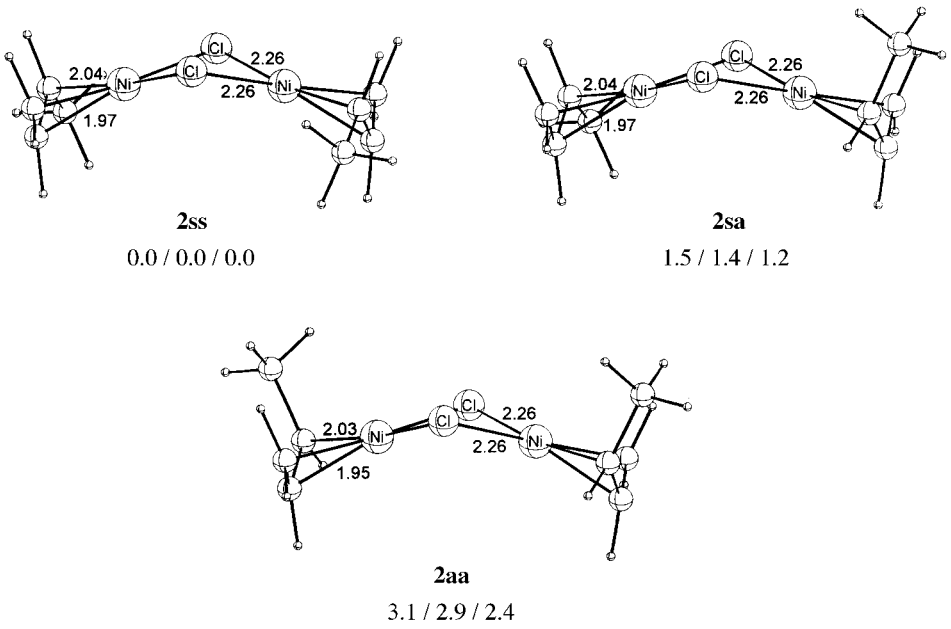

Figure 2. Selected geometric parameters of the optimized structures [Å] of **2** (for **I** as an example) together with relative enthalpies (ΔH in kcal mol^{-1}) for **I/II/III**.

complexes are calculated to be distinctly more stable than the four-coordinate complexes.[21] For butadiene to coordinate in a bidentate fashion, one halide bridge must be cleaved to give a five-coordinate square-pyramidal fragment that contains the butadiene, **2-4**.

The monomeric butadiene complexes show very similar bonding situations to those of the corresponding dimeric complexes in which one Ni–halide bridge is cleaved. The sole difference concerns the anionic ligand in $[RC_3H_4Ni(C_4H_6)X]$, where $X^- = Cl^-$, Br^-, I^- for the monomeric complexes and $X^- = [RC_3H_4NiY_2]^-$, $Y^- = Cl^-$, Br^-, I^- for the dimeric complexes.

Several isomers of monodentate- and bidentate-coordinated dimeric and monomeric π complexes were optimized. The most stable dimeric and monomeric *syn*-butenyl species are displayed in Figure 3, and the complete energetics (ΔE) are given in the Supporting Information (Table 1). Since we are interested in thermodynamic aspects in this section, we shall focus the discussion on the most stable *anti*- and *syn*-butenyl isomers of the different π complexes, for which the enthalpies are summarized in Table 1.

There are some similarities between dimeric and monomeric π complexes: the *syn*-butenyl forms are always thermodynamically more stable than their *anti* counterparts. The *anti*–*syn* gap is of the same order of magnitude for different π complexes and is essentially unaffected by the different halide. Changing the mutual orientation of the reacting butenyl and butadiene moieties has a minor effect on the stability of η^2-complexes, **2-3** and **3**; however, its influence is much more pronounced for η^4-complexes, **2-4** and **4**. For bidentate coordination, the SS orientation is found to give the most stable complexes.

In general, *cis*-butadiene prefers to coordinate in a monodentate fashion in dimeric and monomeric complexes. In the case of dimeric complexes, a large energetic gap is calculated between monodentate, **2-3**, and bidentate, **2-4**, π complexes, in favor of the η^2 species. The gap (ΔH) decreases from 7.0 (**I**) to

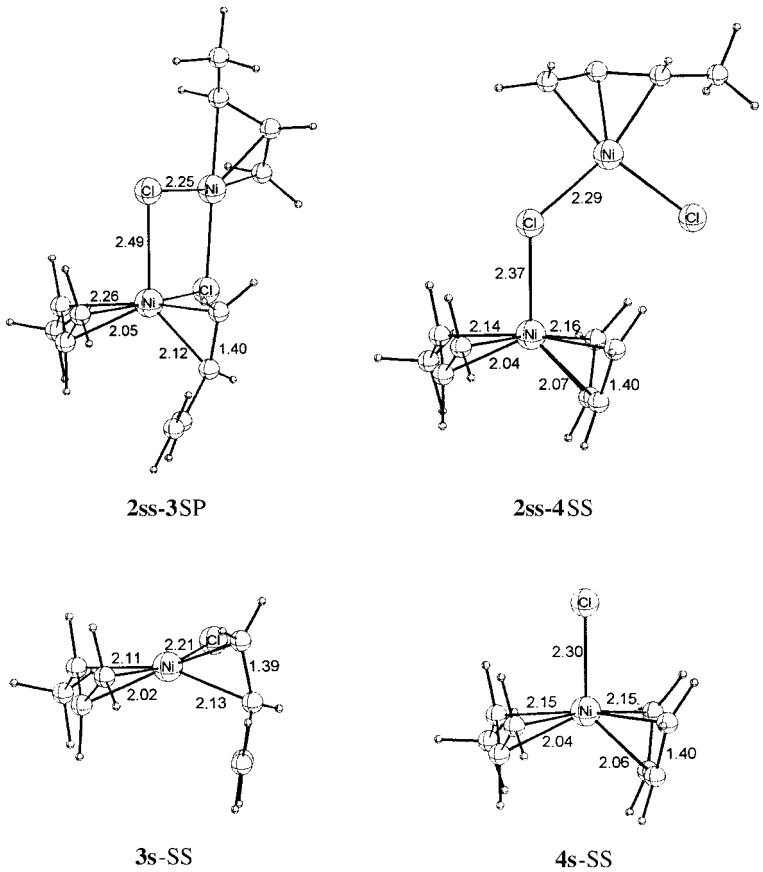

Figure 3. Most stable dimeric and monomeric butadiene π complexes (for **I** as an example).

0947-6539/01/0717-3686 $ 17.50+.50/0 *Chem. Eur. J.* **2001**, *7*, No. 17

Table 1. Formation of butadiene π complexes [ΔH in kcal mol^{-1}] and calculated thermodynamic stability [ΔH in kcal mol^{-1}] of the most stable species of different kinds of dimeric [$Ni(C_4H_7)(C_4H_6)X$] ($X^- = [NiC_4H_7NiY_2]^-$, $Y^- = Cl^-$ (**I**), Br^- (**II**), I^- (**III**)) and monomeric [$Ni(C_4H_7)(C_4H_6)X$] ($X^- = Cl^-$ (**I**), Br^- (**II**), I^- (**III**)) butadiene π complexes.[a–d]

	dimeric-η^2	dimeric-η^4	monomeric-η^2[b]	monomeric-η^4[b]
anti-butenyl	**2as-3**SP	**2as-4**SS	**3a**-SS	**4a**-SS
	3.7/3.3/2.8	10.1/9.2/7.4	7.1/5.5/3.9	9.3/7.0/4.7
syn-butenyl	**2ss-3**SP	**2ss-4**SS	**3s**-SS	**4s**-SS
	0.0/0.0/0.0	7.0/6.0/4.7	4.6/3.3/2.1	6.7/4.4/1.9

[a] Numbers are given for **I/II/III**, with labeling of the species as in Scheme 1. [b] Formation of monomeric complexes according to Equation (5): **2ss-3**SS + BD → **3s**-SS (+ **3s**-SS). [c] **2ss-3**SP was chosen as the reference point. [d] **2ss** + butadiene → **2ss-3**SP is −3.3/−2.5/−2.1.

6.0 (**II**) to 4.7 kcal mol^{-1} (**III**). Thus, our calculations suggests a decreasing stability of the doubly bridged complexes in the order Cl > Br > I. For monomeric complexes, the difference of the thermodynamic driving force to form η^2- and η^4-complexes, (**3** and **4**, respectively), is less pronounced.

The general order of stability calculated for dimeric π complexes is **2ss-3/4** > **2sa-3/4** > **2as-3/4** > **2aa-3/4** (cf. Scheme 1). The *syn*-butenyl isomers, **2ss-3/4** and **2sa-3/4**, are well separated from the *anti*-butenyl isomers, **2as-3/4** and **2aa-3/4**. The configuration of the fragment's butenyl group, where butadiene does not reside, has a lesser influence on the complex π stability with *syn* in favor. Thus, the most stable dimeric η^2/η^4 *syn*- and *anti*-butenyl butadiene complexes capable of achieving chain propagation are **2ss-3/4** and **2as-3/4**, respectively.

The dimeric-η^2 species **2-3**, with **2ss-3**SP as the most stable isomer, are found to be the most stable π complexes occurring under polymerization conditions. **2ss-3**SP is formed in an exothermic process from **2ss** [cf. Eq. (1)] with a reaction enthalpy of ≈2–3 kcal mol^{-1}, which is very similar for all three catalysts. A second butadiene is very weakly coordinated to **2ss-3**SP in an endothermic process that requires ≈1 kcal mol^{-1} (ΔH for **I**, **II**, **III** according to Equation (2)). Thus, we think it unlikely that intermediate bis(butenylnickel(II) halide butadiene) species $C_2X_2(M)_2$ are involved in the polymerization reaction to go along the minimum energy pathway under normal conditions. Therefore, only dimeric monomer complexes of the general formula $C_2X_2(M)$ (**2-3**, **2-4**, **2-5**, **2-6**) will be considered throughout this paper. The dissociative equilibrium between dimeric and monomeric butadiene π complexes is analyzed according to the overall reaction given in Equation (5).

$$C_2X_2(M) + M \rightleftharpoons 2\,CX(M) \qquad (5)$$

From the enthalpies given in Table 1, we conclude that the dissociative equilibrium between different π complexes is largely in direction of the dimeric-η^2 complexes **2-3**. They constitute a thermodynamic sink. For butadiene insertion to occur, bidentate π complexes must be formed (i.e. either **2ss/as-4** or **4s/a**), since they represent the precursors of the insertion transition states (see next paragraph). The energetic gap, relative to **2ss-3**SP, decreases in the order Cl > Br > I. For the η^4-butadiene π complexes, the calculations indicate that both dimeric and monomeric species exist in similar proportions for **I**, whereas for **II** and **III** the monomeric species is more highly populated.

If it is assumed that the chain-propagation step takes place via the monomeric species, the gap (ΔH) between **2ss-3**SP and **4s**-SS is calculated to be 6.7 (**I**), 4.4 (**II**) and 1.9 kcal mol^{-1} (**III**). Application of the Maxwell–Boltzmann statistics (298 *K*) to the enthalpy differences ($\Delta\Delta H$) (4.8 (**I**) and 2.5 kcal mol^{-1} (**II**) higher than for **III**) yields a ratio of ≈1:3300 for chloride and ≈1:70 for bromide, with 1 assumed for iodine **4s**-SS. The calculations clearly show that the thermodynamic population of the catalytically active complexes, which overall is small for the three catalysts, is highest for iodide and decreases in the order I > Br ≫ Cl (of ≈1 order for bromide and of ≈3 orders for chloride, relative to iodide). The moderate activity of **III** as well as the diminishing activity according to **III** > **II** ≫ **I**, verified by experiment, is confirmed by our calculations, provided that insertion is facile and accompanied by barriers which are very similar for all three catalysts.

cis-Butadiene insertion: The chain-propagation step, that is, *cis*-butadiene insertion into the π-allylic Ni–butenyl bond, which occurs in dimeric or monomeric complexes, exhibits a very similar characteristic. The insertion proceeds through two different transition-state configurations, which are distinguished by the *cis*-butadiene orientation. It gives rise to square-pyramidal supine-butadiene and trigonal-bipyramidal prone-butadiene transition states.[22] With regard to the butadiene moiety's distortion the former (i.e. the SS and PS isomers of **2-5** and **5**) are quite late and appear product-like, whereas the latter (i.e. the SP and PP isomers of **2-5** and **5**) are quite early and can be characterized as educt-like. In the transition states of the C^1(butenyl)–C^1(butadiene) bond formation that occurs at distances of ≈2.00–2.30 Å, both reacting parts essentially remain in π coordination (cf. Figure 4). Optimizations going downhill from slightly relaxed transition state structures show that the η^4-butadiene π complexes are the direct precursors of the insertion transition states. The thermodynamically more stable *syn* forms are also more reactive than the corresponding *anti* counterparts. The insertion via square-pyramidal supine-butadiene transition states is disabled by rather large barriers. The chain-propagation step preferably proceeds through trigonal-bipyramidal prone-butadiene transition states.

For insertion to occur along the minimum energy pathway, the butadiene moiety must change its orientation from supine to prone. The energy required for this conversion is almost identical for all three catalysts: it amounts to approximately 6.2 kcal mol^{-1} and 5.7 kcal mol^{-1} for **4s** and **4a**, respectively, (ΔE, cf. Table 2 in the Supporting Information) provided that the barrier associated with this process is low. Figure 4 shows the geometries of the optimized prone-butadiene isomers of **2-5** and **5** together with the relevant structural data. The energetics of the insertion process ($\Delta H^{\neq}$ and $\Delta G^{\neq}$) are summarized in Table 2; however, we will focus the discussion on the Gibbs free energies.

The intrinsic free-activation energy,[23a] across the most stable of the two energetically close-lying prone-butadiene transition states (SP and PP isomers), is nearly identical for

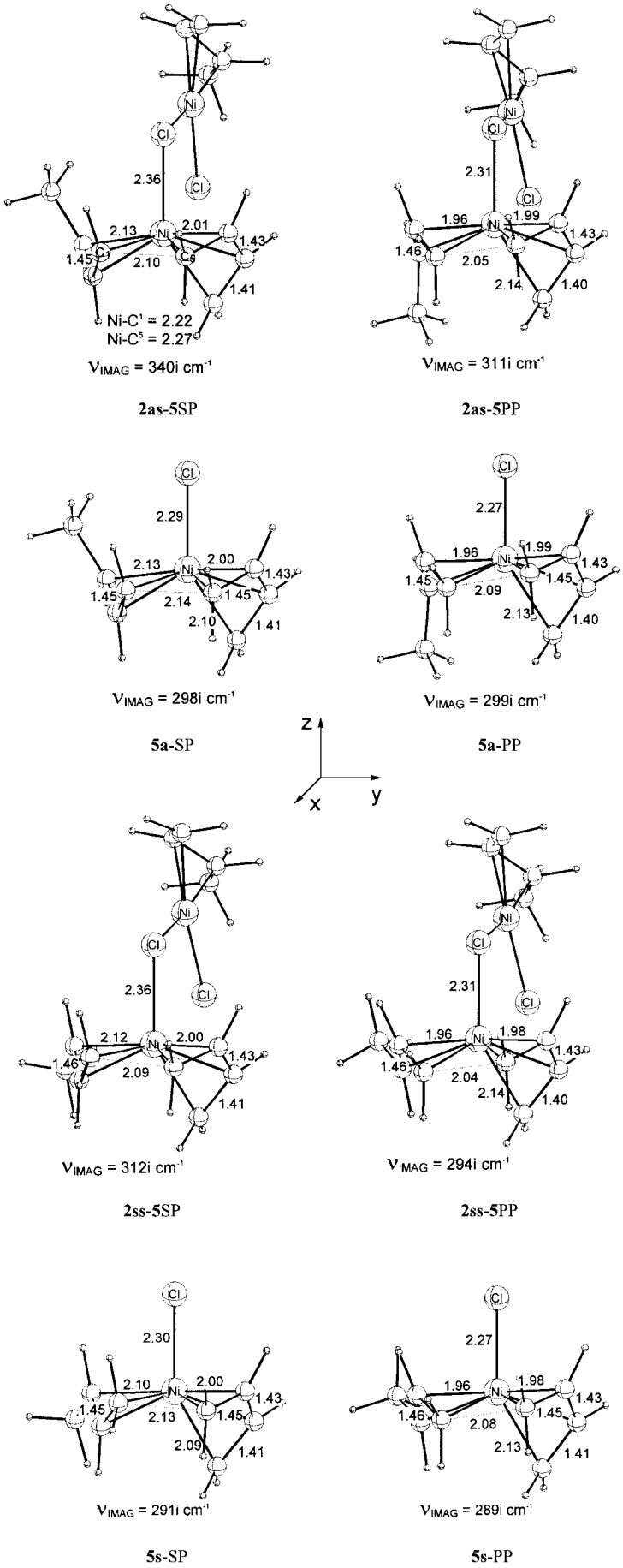

Figure 4. Selected geometric parameters of the optimized structures [Å] of transition states for *cis*-butadiene insertion to occur along the minimum energy pathway for the *cis*-1,4 (k'_{1c}, k_{1c}) and the *trans*-1,4 (k'_{1t}, k_{1t}) generating cycle in dimeric and monomeric butadiene complexes (for **I** as an example).

Table 2. Calculated activation barriers[a, b] (enthalpies ΔH and Gibbs free energies $\Delta G^{\neq}$ in kcal mol^{-1}) for the *cis*-butadiene insertion into the dimeric $[Ni(C_4H_7)(C_4H_6)X]$ $(X^- = [NiC_4H_7NiY_2]^-$, $Y^- = Cl^-$ (**I**), Br^- (**II**), I^- (**III**)) and monomeric $[Ni(C_4H_7)(C_4H_6)X](X^- = Cl^-$ (**I**), Br^- (**II**), I^- (**III**)) complexes. The alternative k_{2c} pathway is added for comparison.

	Intrinsic barrier[23a]	Absolute barrier[23b]
dimeric species		
1,4-*cis* cycle (k'_{1c})	**2as-4**SS → **2as-5**SP/PP	**2ss-3**SP → **2as-5**SP/PP
	17.2/17.3/16.6	27.3/26.5/24.0
	18.4/18.4/17.7	*30.4/28.7/26.2*
1,4-*trans* cycle (k'_{1t})	**2ss-4**SS → **2ss-5**SP/PP	**2ss-3**SP → **2ss-5**SP/PP
	15.9/16.1/15.6	22.9/22.1/19.7
	16.6/16.5/15.9	*25.6/23.9/21.6*
monomeric species		
1,4-*cis* cycle (k_{1c})	**4a**-SS → **5a**-SP/PP	**2ss-3**SP → **5a**-SP/PP
	17.7/17.6/16.9	27.0/24.6/21.6
	19.4/19.0/18.1	*29.7/26.7/23.4*
1,4-*trans* cycle (k_{1t})	**4s**-SS → **5s**-SP/PP	**2ss-3**SP → **5s**-SP/PP
	15.9/16.0/15.6	22.6/20.4/17.5
	17.1/16.8/16.3	*25.2/22.2/19.1*
1,4-*cis* cycle (k_{2c})		**2ss-3**SP → **5′a**-SP
		27.1/26.9/25.0

[a] Numbers are given for **I/II/III**, with labeling of the species as in Schemes 1 and 2, respectively. [b] Numbers in italics are the Gibbs free-activation energies $\Delta G^{\neq}$.

insertion to occur in monomeric or in dimeric complexes. We note that the intrinsic free-energy insertion barrier is apparently in the same order of magnitude for all three catalysts. It is calculated to be ≈16.5 kcal mol^{-1} ($\Delta G^{\neq}$) for *syn*-butenyl forms and ≈18.5 kcal mol^{-1} ($\Delta G^{\neq}$) for the *anti* forms; this indicates a higher intrinsic reactivity of the *syn* species. Therefore, we think it unlikely that kinetic reasons are decisive in the decrease of the catalyst's activity (i.e. I > Br ≫ Cl) observed by experiment. In contrast, the calculations clearly show that the different activity of the three catalysts is mainly thermodynamically determined by the concentration of the catalytically active π complexes.

Though for very similar free-activation energies for insertion to take place in monomeric and in dimeric complexes, the dissociative equilibrium between the π complexes must be taken into account (compare absolute barriers in Table 2) in order to settle the question as to where the insertion is likely to proceed. In accordance with experimental results, we find for iodide and bromide that chain propagation is likely to occur via monomeric complexes. The calculations suggest for chloride a similar probability for insertion to take place in dimeric and monomeric complexes. Therefore, our calculations seem to contradict those observed for **I** with the half-order dependence of the polymerization rate on the catalyst concentration.[9a, 11a,b] As it will be discussed in below, we think it unlikely for chloride that butenyl(halide)(butadiene)Ni^{II} complexes are the catalytically active species. In contrast,

0947-6539/01/0717-3688 $ 17.50+.50/0 *Chem. Eur. J.* **2001**, *7*, No. 17

for chloride we would suggest that chain propagation takes place via highly reactive cationic polybutadienyl(butadiene)-Ni^{II} complexes. They are formed by an unsymmetrical bond rupture of the dimeric butadiene π complexes, thus giving ionic products according to Equation (6).

$$C_2X_2(M)_2 \rightleftharpoons C(M)^+ + CX_2^- + M \quad (6)$$

Propagation along this alternative reaction pathway, which should also be passed through with a certain probability for bromide, is consistent with the observed half-order dependence of the overall polymerization rate on the catalyst concentration.[9c, 11a,b]

Passage via **5s** and **5a** following the k_{1t} and k_{1c} channels leads to the kinetic insertion products **6a**-*trans* and **6a**-*cis*, respectively, with an *anti*-butenyl chain elongated by a new *trans* (k_{1t}) or *cis* (k_{1c}) double bond. The thermodynamic driving force (ΔH) of butadiene insertion relative to **4s**-SS and **4a**-SS is very similar for all three catalysts. It is approximately 9.7 kcal mol^{-1} and 12.0 kcal mol^{-1} along the *trans*-1,4 and the *cis*-1,4 generating cycle (please note that the intrinsic energy to extent the polymer chain by an additional C_4 unit in subsequent propagation cycles (see Computational Model and Methods) is excluded in Scheme 1). Together with the monomeric π species, which is not involved in the insertion process, **6a**-*trans* and **6a**-*cis* dimerize back to **2sa-3**SP as the most stable species after *anti* insertion, with either a new *trans* or *cis* C_4 unit of the polymer chain.

Our calculations show the dimeric η^2-butadiene π-complex **2ss-3**SP to be the most stable species under polymerization conditions (cf. Scheme 1), which therefore must be regarded as the resting state of the catalyst.

anti–syn Isomerization: The isomerization of the π-butenyl group in cationic and neutral Ni^{II} complexes most likely takes place by means of a η^3-π → η^1-σ-C^3 butenyl group conversion, followed by internal rotation of the vinyl group around the C^2—C^3 single bond.[24] The occupation of the single vacant coordination site occurring in this process, thus keeping the coordination number of the nickel center as five, is a prerequisite of a facile isomerization process. It is reasonable to assume that isomerization occurs when starting from butadiene π complexes. The isomerization step preferably proceeds via trigonal-bipyramidal transition states, regardless of whether they are dimeric or monomeric species.[22]

Several isomers of dimeric and monomeric σ-C^3-butenyl complexes were located and the most stable are displayed in Figure 5. They represent the rotational transition structures for the conversion of *anti*-butenyl forms (arising from the kinetic insertion products) into *syn*-butenyl forms that were passed through along the minimum energy pathway in dimeric, **2-7**, or in monomeric, **7**, complexes (for the sequence of complexes involved in isomerization, see Table 3). The dimeric species **2-7a** and **2-7s** differ in the *anti* and *syn* structure of the fragment's butenyl group which is not involved in the isomerization process. **2-7** and **7** are confirmed to have only one imaginary frequency. The corresponding normal mode represents a rotational displacement around the C^2—C^3 single bond. In the trigonal-bipyramidal transition states, the σ-C^3-butenyl group occupies an axial position. For monomeric species, we have assumed the coordination of the growing polymer chain in order to make the nickel center coordinatively saturated.[25a,b] Our calculations give no indication for a participation of the polymer chain for isomerization to occur in dimeric complexes. In contrast to **7**, the dimeric σ-butenyl species **2-7** are stabilized by a change in

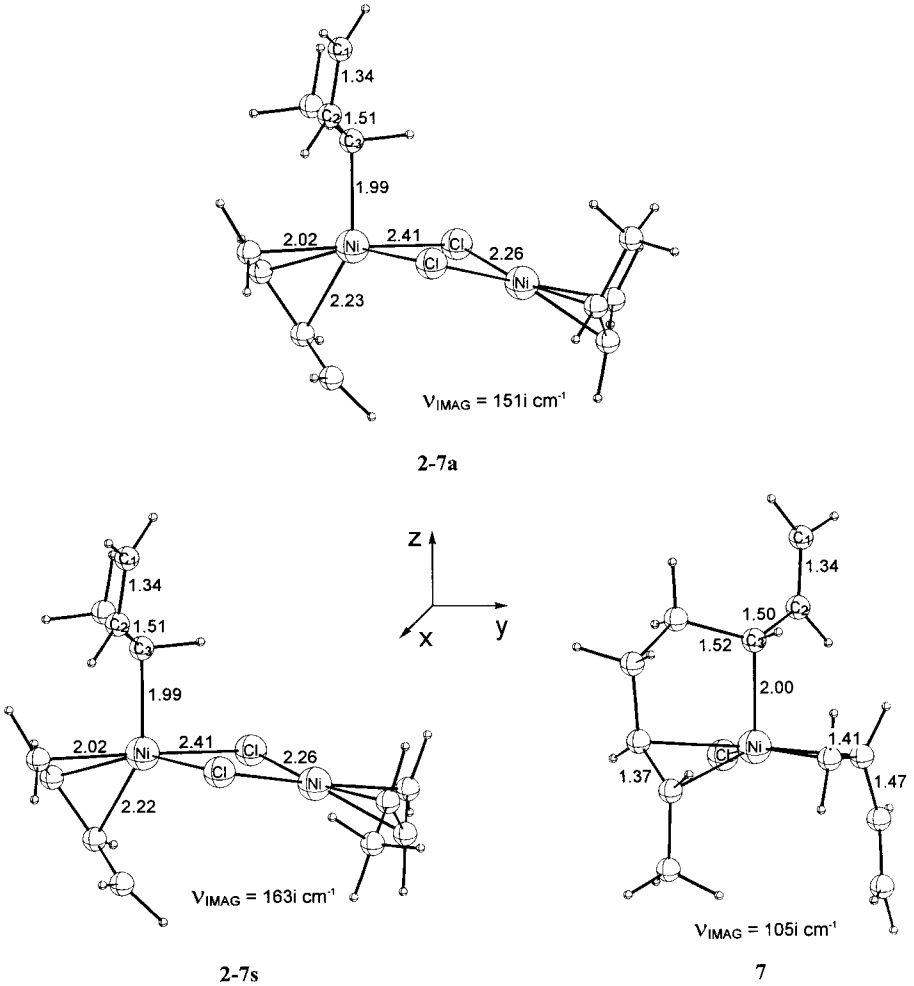

Figure 5. Selected geometric parameters of the optimized structures [Å] of transition states for *anti–syn* isomerization to occur in dimeric and monomeric butadiene complexes (for **I** as an example).

Table 3. Calculated activation barriers[a,b] (enthalpies $\Delta H^{\neq}$ and Gibbs free energies $\Delta G^{\neq}$ in kcal mol^{-1}) for *anti–syn* isomerization to occur in dimeric $[Ni(C_4H_7)(C_4H_6)X]$ ($X^- = [NiC_4H_7NiY_2]^-$, $Y^- = Cl^-$ (**I**), Br^- (**II**), I^- (**III**)) and monomeric $[Ni(C_4H_7)(C_4H_6)X]$ ($X^- = Cl^-$ (**I**), Br^- (**II**), I^- (**III**)) complexes.

	Intrinsic barrier[23c]	Absolute barrier[23d]
dimeric species	**2aa-3**SP → **2-7a** → **2sa-3**SP	**2sa-3**SP → **2-7a** → **2aa-3**SP
	17.5/17.4/17.4	21.1/20.8/20.1
	18.2/18.1/18.5	*22.3/22.0/21.5*
	2as-3SP → **2-7s** → **2ss-3**SP	**2sa-3**SP → **2as-3**SP → **2-7s** → **2ss-3**SP
	17.6/17.6/17.5	19.4/19.2/18.9
	18.3/18.5/18.7	*20.6/20.5/20.7*
monomeric species	**3a**-SP → **7** → **3s**-SS	**2sa-3**SP → **7** → **3s**-SS
	20.4/20.6/21.1	25.6/24.4/23.6
	22.3/22.3/22.8	*26.9/25.8/25.1*

[a] Numbers are given for **I/II/III**, with labeling of the species as in Scheme 1. [b] Numbers in italics are the Gibbs free-activation energies $\Delta G^{\neq}$.

butadiene's mode from η^2 to almost η^4, while both nickel–halide bridges are retained (cf. Figure 5).

The conversion between dimeric π complexes **2sa-3/4** and **2as-3/4** (cf. Scheme 1) most likely takes place by dissociative displacement of butadiene from one fragment and subsequent reassociation with the other fragment. This process is expected to take place without a significant kinetic barrier. Therefore, the population of *anti* and *syn* complexes is kinetically determined by the isomerization barriers via **2-7** and **7**.

The energetics of the isomerization process ($\Delta H^{\neq}$ and $\Delta G^{\neq}$) are summarized in Table 3. The intrinsic free-energy barrier[23c] is nearly identical for all three catalysts, similar to the situation found for chain propagation. It is calculated to be approximately 18.3 (almost identical via **2-7a** and **2-7s**) and 22.5 kcal mol^{-1} ($\Delta G^{\neq}$) for isomerization to occur in dimeric and monomeric complexes, respectively. When taking the dissociative equilibrium between different kinds of butadiene complexes into account, the gap between **2-7s** and **7** increases to more than 4.5 kcal mol^{-1} ($\Delta G^{\neq}$), in favor of the dimeric species. Therefore, the calculations predict that *anti–syn* isomerization most likely takes place in dimeric complexes through **2-7s** as the preferred route.

Comparison of free-activation energies for *cis*-butadiene insertion and for *anti–syn* isomerization: The absolute free-energy activation barrier[23e] for competitive insertion pathways and for isomerization are compared to find out which of both crucial processes must be regarded as rate-determining.

For polymerization to occur along the minimum energy pathway, the free-energy insertion barrier is calculated to be 25.2/29.7 (**I**), 22.2/26.7 (**II**), and 19.1/23.4 kcal mol^{-1} (**III**) (cf. Table 2) according to k_{1t}/k_{1c}, and the free-activation energy for isomerization is 20.6 (**I**), 20.5 (**II**), and 20.7 kcal mol^{-1} (**III**) (cf. Table 3). Thus, the calculations suggest the isomerization to be more facile than insertion for chloride and bromide. For iodide, our calculations seem to disagree with experimental findings which concluded that isomerization is much more rapid than insertion. However it must be emphasized that a correlation between calculated barriers and relative rates is not strictly possible because of the different rate laws of both processes. Since the difference in the free-activation barrier for insertion and isomerization is predicted to be only 1.6 kcal mol^{-1}, we think the calculations are not in conflict with experiment, so that isomerization is more rapid than insertion for **III**. We conclude that, for all three catalysts, *cis*-butadiene insertion is rate-determining, because the free-activation energy for isomerization for **I** and **II** is distinctly below that of monomer insertion.

Since $k_{a/s}{}^{p} \gg k_{1c}$, k_{1t} is valid, on account of the Curtin–Hammett principle,[26] the stereoselectivity is solely controlled by the difference in free energies of the transition-state species that were passed through along the minimum pathway of both competing *cis*-1,4 (following the k_{1c} pathway) and *trans*-1,4 (following the k_{1t} pathway) generating cycles (compare absolute barriers in Table 2). The calculations clearly show that the *trans*-1,4 generating cycle is most probably passed through for all three catalysts, because of a higher *syn* reactivity, but with an activity that decreases in the order **III** > **II** ≫ **I**. The *anti*-insertion transition states (**5a**-SP/PP) are energetically well-separated from the *syn* forms (**5s**-SP/PP) by ≈4.5 kcal mol^{-1} ($\Delta\Delta G^{\neq}$), in favor of the *syn* forms, for all three catalysts. Therefore, we consider the generation of a *cis*-1,4 polymer following the k_{1c} pathway as highly unlikely in all cases, since the *anti* forms should be distinctly less reactive. The kinetically determined polymer of predominantly *trans*-1,4 structure should not possess any stereoregularity within the methylene groups on account of to a very similar reactivity of SP and PP transition state isomers (see the Supporting Information).

Our calculations show some characteristics common for all three catalysts, which are important for the elucidation of the mechanism of stereoregulation. First, butadiene insertion into the π-butenylnickel(II) bond is very likely to proceed commencing from s-*cis* butadiene (π-allyl insertion mechanism, *anti* insertion). Second, the *syn* forms are distinctly more reactive than the *anti* forms. Third, isomerization is much more rapid than butadiene insertion, thus the insertion is rate-determining.

The formation of a stereoregular *trans*-1,4 polymer by **III** can be readily explained. The high *cis*-1,4 selectivity experimentally verified for **I**, however, cannot be understood from the insertion that occurred through the k_1 channel in butenyl(halide)(butadiene)nickel(II) complexes. In our opinion, the extremely low catalytic activity of **I** suggests an essentially thermodynamic control of the activity and *cis–trans* selectivity by making the k_2 channel accessible (Scheme 2). The dissociation of dimeric butadiene complexes **2-3**, **2-4** with participation of the monomer can take place in two different ways. First, in a symmetrical fashion to give two neutral monomeric butenyl(halide)(butadiene)nickel(II) complexes **3** and **4** (cf. Equation (5)); thus opening the k_1 channel. Second, the halide bridges can be broken unsymmetrically to yield ionic species (cf. Equation (6)); namely, cationic polybutadienyl(butadiene) complexes **4′** by coordination of the next double bond in the growing chain and the corresponding counteranions $X^- = [RC_3H_4NiY_2]^-$, $Y^- = Cl^-$, Br^-, I^-. The k_2 channel would be opened by **4′a** and **4′s**, which catalyze the generation of *cis*-1,4 polymer units according to the k_{2c} pathway.[8c]

0947-6539/01/0717-3690 $ 17.50+.50/0 *Chem. Eur. J.* **2001**, *7*, No. 17

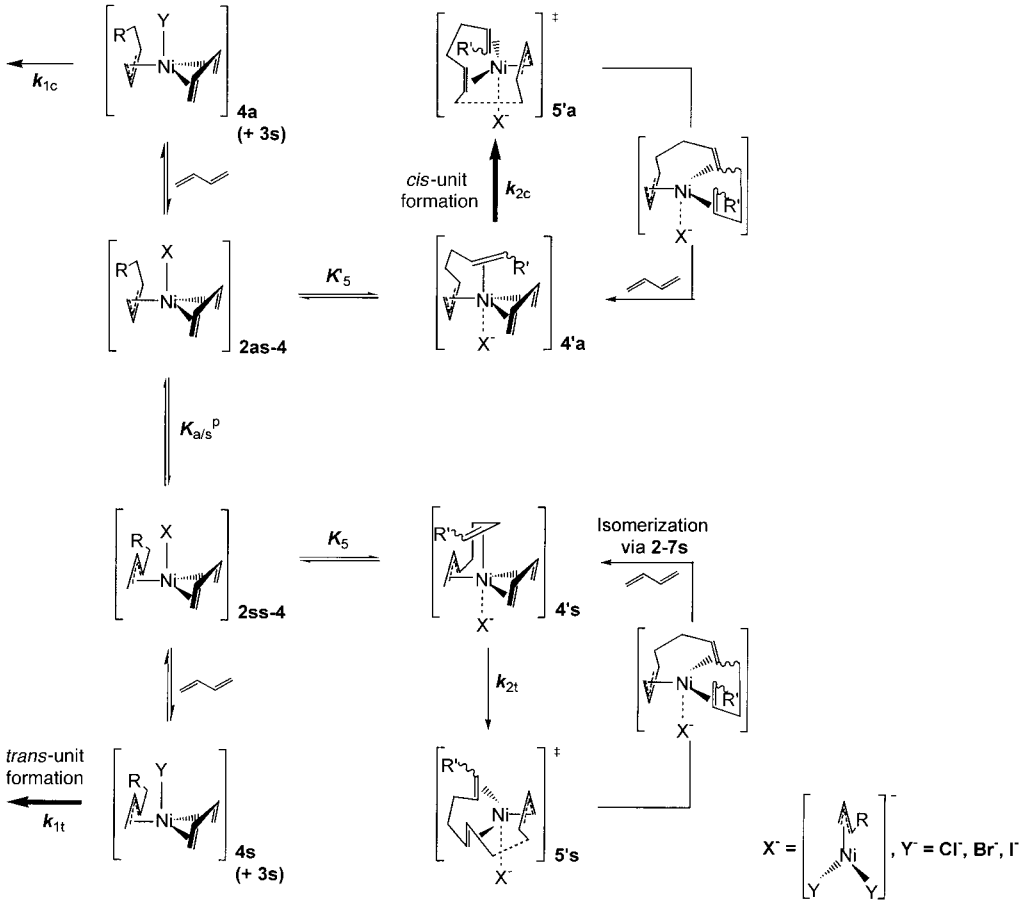

Scheme 2. Two possible reactions channels for the 1,4-polymerization of butadiene mediated by neutral dimeric allylnickel(II) halides either via butenyl(halide)(butadiene)nickel(II) complexes **4a**/**4s** (k_1) or via polybutadienyl(butadiene)nickel(II) complexes **4′a**/**4′s** (k_2) where $X^- = [RC_3H_4NiY_2]^-$, $Y^- = Cl^-$, Br^-, I^-.

The dissociative equilibrium between **2-4** and **4′** (K_5, K'_5 in Scheme 2) is largely dependent on the electronegativity of the halide, which allows the coordinating polymer chain to compete coordinatively with the anion ligand more or less. Since the electronegativity of the halides and, therefore, the acceptor strength of the Ni^{II} center decreases from chlorine to iodine, the complex formation tendency of **4′** should be at its highest for **I**. For all three catalysts, the k_1 channel is calculated to be energetically preferred with respect to the k_2 channel. The energetic gap between alternative pathways ($\Delta H^{\neq}$ k_{1t} versus k_{2c}), however, decreases in the order **III** (7.5 kcal mol^{-1}) < **II** (6.5 kcal mol^{-1}) < **I** (4.5 kcal mol^{-1}) (cf. Table 2, Figure 6).[27] Although the *cis*-1,4 cycle is still energetically more expensive than the *trans*-1,4 cycle, the calculations suggest that the k_{2c} pathway is most feasible for **I** and almost unlikely for **III**.

Therefore, the production of a stereoregular *cis*-1,4 polymer by the chloride catalyst can be explained if, under thermodynamic control, the *cis*-1,4 cycle (k_{2c} pathway) is passed through. Although **4′** are only sparsely populated, their higher reactivity (compared with that of **4**) may give rise to the extremely low catalytic activity observed for **I**.[10d, 11a] The preestablished *anti*–*syn* equilibrium can be

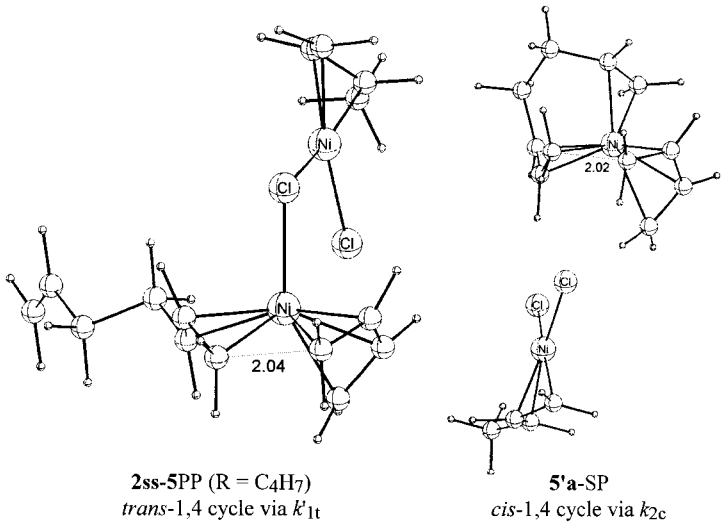

2ss-5PP (R = C_4H_7)
trans-1,4 cycle via k'_{1t}

5'a-SP
cis-1,4 cycle via k_{2c}

Figure 6. Selected geometric parameters of the optimized structure [Å] of the transition state for *cis*-butadiene insertion to occur along the k_{1t} and k_{2c} pathways for production of *trans*-1,4 and *cis*-1,4 polymer units, respectively (for **I** as an example).

  0947-6539/01/0717-3691 $ 17.50+.50/0

regarded as being attained (via **2-7s**) and the *cis*-1,4 selectivity could arise from the higher reactivity of **4′a** relative to that of **4′s**, which is amplified under the influence of a weakly coordinating anion $[RC_3H_4NiY_2]^-$, with $Y^- = Cl^-, Br^-, I^-$. The k_{2c} channel is disabled for **III** because of the negligible population of catalytically active π complexes **4′**. Thus, a polymer with a predominantly *trans*-1,4 structure is generated according to k_{1t} for the moderately active iodide catalyst. Butadiene insertion to occur with a similar probability via k_{1t} and k_{2c} can be assumed to explain the statistical *cis*/*trans* equibinary polymer given by the bromide catalyst.

Conclusion

We have studied the mechanism of stereoregulation of 1,4-polymerization of butadiene with the neutral dimeric allylnickel(II) halides $[Ni(C_3H_5)X]_2$ as the catalyst. We have investigated monomer π complex formation, symmetrical and asymmetrical splitting of dimeric π complexes, *anti*–*syn* isomerization, and also competitive routes for chain propagation occurring in dimeric and monomeric butenyl(halide)-(butadiene)nickel(II) complexes $[RC_3H_4Ni(C_4H_6)X]$.

From the present research, the following conclusions could be drawn: in the starting material, in the absence of butadiene, the *syn* configuration of the butenyl group is thermodynamically more stable than the *anti* configuration for all three catalysts, thus **2ss** is predominant.

Commencing with the neutral dimeric allylnickel(II) halides, the corresponding dimeric butenylnickel(II) complexes **2** are formed after a short initialization period.[9c] Subsequently, dimeric and monomeric butadiene π complexes, with either monodentate or bidentate coordination of butadiene, are formed with butadiene. All of them are in equilibrium. The dissociative equilibrium between dimeric and monomeric species involving butadiene is assumed to be very mobile and can therefore be regarded as always being attained. The conversion of *anti*- into *syn*-butenyl forms, however, is accompanied by a significant kinetic barrier. The *syn* forms are always thermodynamically more stable than the *anti* counterparts under polymerization conditions. Butadiene uptake preferentially takes place through monodentate coordination in dimeric complexes.

The dimeric η^2-π complexes, **2-3**, are the most stable species occurring under polymerization conditions and constitute a thermodynamic sink. The stability of **2-3** decreases in the order Cl > Br > I, with the most electrophilic chloro complexes being the most stable. The calculations clearly show that the thermodynamic population of the catalytically active η^4-butadiene complexes, which overall is small for the three catalysts, is highest for iodide and decreases in the order I > Br ≫ Cl. Thus, the moderate activity of **III** as well as the diminishing activity according to **III** > **II** ≫ **I**, verified by experiment, is confirmed by our calculations, provided that insertion is facile and accompanied by barriers which are very similar for all three catalysts.

Chain propagation occurs by *cis*-butadiene insertion into the *syn*-butenylnickel(II) bond. The insertion proceeds in monomeric complexes through trigonal-bipyramidal prone-butadiene transition states which always yield *anti*-butenyl products under kinetic control. The thermodynamically more stable *syn* forms are also more reactive than the corresponding *anti* counterparts. The intrinsic free-energy insertion barriers of approximately 16.5 and 18.5 kcal mol^{-1} for *syn* and *anti* forms, respectively, are very similar for all three catalysts. Also, the thermodynamic driving force (ΔH) of the propagation step is in the same order of magnitude for the three catalysts. It is approximately 9.7 and 12.0 kcal mol^{-1} along the *trans*-1,4 and *cis*-1,4 production cycle.

Isomerization most likely takes place in dimeric complexes through trigonal-bipyramidal σ-C^3-butenyl transition states, with **2-7s** energetically preferred, which constitute the internal rotation of the vinyl group around the C^2–C^3 single bond. The intrinsic free-energy activation barrier associated with this process is ≈18.5 kcal mol^{-1}, which is almost identical for all three catalysts.

The following steps are passed through along the energetically most favorable reaction pathway for generating *trans*-1,4 polymer units (cf. Figure 7): commencing with the most stable *cis*-butadiene π complex **2ss-3**, **2ss-4** is formed. After uptake of an additional monomer and subsequent dissociation **3s** (+ **3s**) and **4s** (+ **3s**) are formed. Complex **4s** undergoes the required conversions to pass over a moderate barrier to give **5s** (following k_{1t}) and decays into the kinetic *anti* product **6a**-*trans* (see Scheme 1). With the **3s** species, not involved in the insertion process, **6a**-*trans* dimerizes back via **2as-3** to **2sa-3**. **2sa-3** are formed as the most stable species after *anti* insertion, as long as isomerization does not occur. Since **2sa-3** is readily converted into **2as-3**, isomerization can take place via **2-7s** and the catalytic cycle is closed. For production of a *cis*-1,4 polymer, the following sequence of species is involved: **2as-3** → **2as-4** → **3a** (+ **3s**) → **4a** (+**3s**) → **5a** (+ **3s**) → **6a**-*cis* (+ **3s**) → **2as-3**.

From the condensed free-energy profile for **III** (Figure 7), it is evident that the *cis*-1,4 pathway following k_{1c} is disabled for energetic reasons as long as the chain-propagation step is rate-determining. Experiment determined a chain-propagation barrier of $\Delta G^{\neq} = 21$ kcal mol^{-1} for the iodide catalyst.[9b] In good agreement with this experimental value, we calculated the free-activation barrier along the k_{1t} pathway to be 19.1 kcal mol^{-1}.

There are some common features for all three catalysts which are important for elucidating the mechanism of stereoregulation. First, chain propagation occurs by *cis*-butadiene insertion into the π-butenylnickel(II) bond. Second, the *syn* forms are distinctly more reactive than the *anti* forms. Third, the chain-propagation step is rate-determining for the entire polymerization process, and the preestablished *anti*–*syn* equilibrium can always be regarded as attained. The isomerization, therefore, is not decisive in the generation of a *cis*-1,4 or *trans*-1,4 polymer. The ratio of *cis* and *trans* units in the polymer chain is determined by the difference in the absolute reactivity of the *syn*- and *anti*-butenyl π complexes.

Accordingly, under kinetic control, neutral dimeric allylnickel(II) halides catalyze the formation of *trans*-1,4 polymer units following the k_{1t} pathway with a strongly decreasing activity in the order **III** > **II** ≫ **I**. This agrees with the experimental verification of the allylnickel iodide as a

0947-6539/01/0717-3692 $ 17.50+.50/0 *Chem. Eur. J.* **2001**, *7*, No. 17

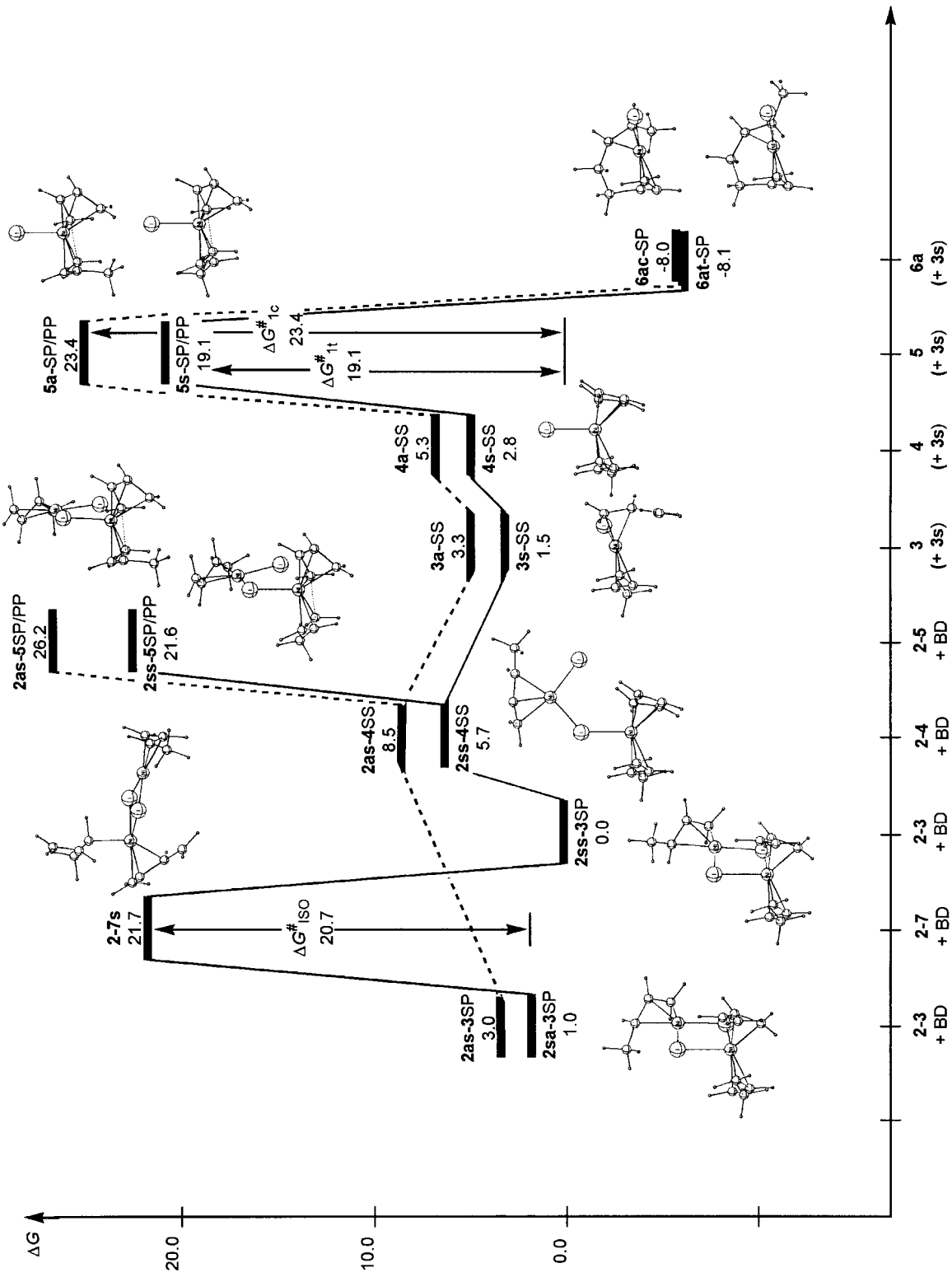

Figure 7. Condensed free-energy profile for the *trans*-1,4 (——) and the *cis*-1,4 (----) production cycle of the $[Ni(RC_3H_4)I]_2$ (**III**)-catalyzed butadiene-polymerization reaction occurring via butenyl(halide)-(butadiene)nickel(II) complexes (cf. Scheme 1 and the text for the labeling of the complexes).

moderately active catalyst that yields almost exclusively a stereoregular *trans*-1,4-polymer. Experiment determined no stereoregularity within the methylene groups of the *trans*-1,4-polymer.[28] This is confirmed by our calculations.

The production of a stereoregular *cis*-1,4-polybutadiene with allylnickel chloride can only be explained by making the k_{2c} channel accessible as a result of the formation of polybutadienyl(butadiene) complexes which is accompanied by coordination of the next double bond in the polymer chain to the Ni^{II} center. A similar probability for butadiene insertion to occur by routes k_{1t} and k_{2c} can be assumed to help understand the formation of the statistical *cis*/*trans* equibinary polymer afforded by the bromide catalyst.

The differences in the catalytic activity and the *cis*–*trans* selectivity of the allylnickel(II) halides are entirely thermodynamically determined by the different ability to form reactive butenyl(halide)(butadiene)nickel(II) complexes (**4**) or polybutadienyl(butadiene)nickel(II) π complexes (**4′**), depending on the electronegativity of the halide.

Acknowledgements

S.T. is indebted to Prof. Dr. R. Ahlrichs (University of Karlsruhe, Germany) for making the latest version of TURBOMOLE available. We acknowledge excellent service by the computer centers URZ Halle and ZIB Berlin.

[1] a) *Applied Homogeneous Catalysis with Organometallic Complexes* (Eds.: B. Cornils, W. A. Herrmann), VCH, Weinheim, Germany, **1996**; b) L. Porri, A. Giarrusso in *Comprehensive Polymer Science, Vol. 4* (Eds.: G. C. Eastmond, A. Ledwith, S. Russo, B. Sigwalt), Pergamon, Oxford, U.K., **1989**, Part II, pp. 53–108.

[2] R. T. La Flair, U. U. Wolf in *Ullmann's Encyclopedia of Industrial Chemistry, 5th Ed., Vol. A23*, Verlag Chemie, Weinheim, Germany, **1993**, pp. 273–282.

[3] P. Pino, U. Giannini, L. Porri in *Encyclopedia of Polymer Science and Engineering, 2nd Ed., Vol. 8*, Wiley, New York, **1987**, pp. 147–220.

[4] M. I. Lobach, V. A. Kormer, I. Yu. Tsereteli, G. P. Kondoratenkov, B. D. Babitskii, V. I. Klepikova, *J. Polym. Sci. Polym. Lett.* **1971**, *9*, 71.

[5] R. Warin, P. Teyssié, P. Bourdaudurq, F. Dawans, *J. Polym. Sci. Polym. Lett.* **1973**, *11*, 177.

[6] a) P. Cossee, P. in *Stereochemistry of Macromolecules*, *Vol. 1* (Eds.: A. D. Ketley) Marcel Dekker, New York, **1967**, p. 145; b) E. J. Arlman, *J. Catal.* **1966**, *5*, 178.

[7] a) R. Taube, J.-P. Gehrke, R. Radeglia, *J. Organomet. Chem.* **1985**, *291*, 101; b) R. Taube, J.-P. Gehrke, P. Böhme, *Wiss. Zeitschr. Tech. Hochschule Leuna-Merseburg* **1987**, *39*, 310; c) R. Taube, U. Schmidt, J.-P. Gehrke, P. Böhme, J. Langlotz, S. Wache, *Makromol. Chem. Macromol. Symp.* **1993**, *66*, 245; d) R. Taube, H. Windisch, S. Maiwald, *Makromol. Chem. Macromol. Symp.* **1995**, *89*, 393; e) R. Taube, G. Sylvester, in *Applied Homogeneous Catalysis with Organometallic Complexes* (Eds.: B. Cornils, W. A. Herrmann), VCH: Weinheim, Germany, **1996**, 280–317.

[8] a) S. Tobisch, H. Bögel, R. Taube, *Organometallics* **1996**, *15*, 3563; b) S. Tobisch, H. Bögel, R. Taube, *Organometallics* **1998**, *17*, 1177; c) S. Tobisch, R. Taube, *Organometallics* **1999**, *18*, 5204.

[9] a) G. Wilke, B. Bogdanovic, P. Hardt, P. Heimbach, W. Keim, M. Kröner, W. Oberkirch, K. Tanaka, E. Steinrucke, D. Walter, H. Zimmermann, *Angew. Chem.* **1966**, *78*, 157; *Angew. Chem. Int. Ed. Engl.* **1966**, *5*, 151; b) L. Porri, G. Natta, M. C. Gallazzi, *J. Polym. Sci., Part C* **1967**, *16*, 2525; c) J. F. Harrod, L. R. Wallace, *Macromolecules* **1969**, *2*, 449; d) J. F. Harrod, L. R. Wallace, *Macromolecules* **1972**, *5*, 682; e) T. Matsumoto, J. Furukawa, *J. Polym. Sci., Part B* **1967**, *5*, 935; f) T. Matsumoto, J. Furukawa, *J. Macromol. Sci. Chem.* **1972**, *A6*, 281.

[10] a) B. A. Dolgoplosk, B. D. Babitskii, V. A. Kormer, M. I. Lobach, E. T. Tinyakova, *Dokl. Akad. Nauk SSSR* **1965**, *164*, 1300; b) V. M. Frolov, A. V. Volkov, O. P. Parenago, B. A. Dolgoplosk, *Dokl. Akad. Nauk SSSR* **1967**, *177*, 1359; c) V. A. Kormer, B. D. Babitskii, M. I. Lobach, N. N. Chesnokova, *J. Polym. Sci., Part C*, **1969**, *16*, 4351; d) V. A. Kormer, B. D. Babitskii, M. I. Lobach, *Adv. Chem. Ser.* **1969**, *91*, 306; e) V. I. Klepikova, G. P. Kondratenkov, V. A. Kormer, M. I. Lobach, L. A. Churlyaeva, *J. Polym. Sci. Polym. Lett.* **1973**, *11*, 193; f) V. I. Klepikova, G. B. Erusalimskii, M. I. Lobach, L. A. Churlyaeva, V. A. Kormer, *Macromolecules* **1976**, *9*, 217; g) V. A. Kormer, M. I. Lobach, V. I. Klepikova, B. D. Babitskii, *J. Polym. Sci. Polym. Lett.* **1976**, *14*, 317; h) M. I. Lobach, V. A. Kormer, *Macromolecules* **1977**, *10*, 572; i) N. N. Druz, A. V. Zak, M. I. Lobach, V. A. Vasiliev, V. A. Kormer, *Europ. Polym. J.* **1978**, *14*, 21.

[11] a) M. A. Lazutkin, V. A. Vashkevich, S. S. Medvevdev, V. N. Vasiliev, *Dokl. Akad. Nauk* **1967**, *175*, 859; b) A. M. Lazutkin, A. I. Kadantseva, V. A. Vashkevich, S. S. Medvedev, *Vysokomol. Soed.* **1970**, *12B*, 635; c) A. I. Lazutkina, L. J. Alt, A. Matveeva, A. M. Lazutkin, Y. I. Ermakov, *Kinet. Katal.* **1971**, *12*, 1162.

[12] a) H. Lehmkuhl, T. Keil, R. Benn, A. Rufinska, C. Krüger, J. Poplawska, M. Bellenbaum, *Chem. Ber.* **1988**, *121*, 1931; b) C. A. Tolman, *J. Am. Chem. Soc.* **1970**, *92*, 6777.

[13] D. E. Robert, *J. Res. Natl. Bur. Stand.* **1950**, *44*, 221.

[14] a) J. Andzelm, E. Wimmer, *Physica B* **1991**, *172*, 307; b) J. Andzelm, in *Density Functional Methods in Chemistry*, (Eds.: J. Labanowski, J. Andzelm), Springer, Berlin, **1991**; DGauss and UniChem are software packages available from Molecular Simulations Inc..

[15] a) M. Häser, R. Ahlrichs, *J. Comput. Chem.* **1989**, *10*, 104; b) R. Ahlrichs, M. Bär, M. Häser, H. Horn, C. Kölmel, *Chem. Phys. Lett.* **1989**, *162*, 165.

[16] a) P. A. M. Dirac, *Proc. Cambridge Philos. Soc.* **1930**, *26*, 376; b) J. C. Slater, *Phys. Rev.* **1951**, *81*, 385; c) S. H. Vosko, L. Wilk, M. Nussiar, *Can. J. Phys.* **1980**, *58*, 1200; d) A. D. Becke, *Phys. Rev.* A **1988**, *38*, 3098; e) J. P. Perdew, *Phys. Rev. B* **1986**, *33*, 8822.

[17] a) DGauss basis set library; b) N. Godbout, D. R. Salahub, J. Andzelm, E. Wimmer, *Can. J. Chem.* **1992**, *70*, 560; c) A. H. J. Wachters, *J. Chem. Phys.* **1970**, *52*, 1033; d) P. J. Hay, *J. Chem. Phys.* **1977**, *66*, 4377; e) A. Bergner, M. Dolg, W. Küchle, H. Stoll, H. Preuß, *Mol. Phys.* **1993**, *80*, 1431; f) TURBOMOLE basis set library.

[18] H. Yasuda, A. Nakamura, *Angew. Chem.* **1987**, *99*, 745, *Angew. Chem. Int. Ed. Engl.* **1987**, *16*, 723.

[19] a) *Mechanisms in Inorganic Chemistry*, (Eds.: F. Basolo, R. G. Pearson), Thieme, Stuttgart, Germany, **1973**; b) M. L. Tobe in *Comprehensive Coordination Chemistry, Vol. I*, (Eds.: G. Wilkinson, R. D. Gillard, J. A. McCleverty), Pergamon Press, New York, **1987**, 281–384; c) R. J. Cross, *Chem. Soc. Rev.* **1985**, *14*, 197; d) R. J. Cross, *Adv. Inorg. Chem.* **1989**, *34*, 219.

[20] a) J. R. Johnson, P. S. Tully, P. B. McKenzie, M. Sabat, *J. Am. Chem. Soc.* **1991**, *113*, 6172; b) M. R. Churchill, A. O'Brien, *Inorg. Chem.* **1967**, *6*, 1386.

[21] The energetic gap between them amounts to 9.0, 8.5, and 7.5 kcal mol^{-1} (ΔE) for **2ss-3** of **I**, **II**, and **III**, respectively.

[22] For dimeric complexes it concerns the fragment which contains *cis*-butadiene.

[23] a) Intrinsic insertion barriers are defined as the energetic difference between the most stable isomers of the insertion transition states and the corresponding η^4-butadiene π complexes, namely **2ss-4**SS → **2ss-5**SP/PP and **2as-4**SS → **2as-5**SP/PP for dimeric *syn*- and *anti*-butenyl species; **4s**-SS → **5s**-SP/PP and **4a**-SS → **5a**-SP/PP for monomeric *syn*- and *anti*-butenyl species. b) Absolute insertion barriers are defined as the energetic difference between the most stable isomer of the insertion transition states and the overall most stable π complex, namely **2ss-3**SP → **2ss-4**SS → **2ss-5**SP/PP and **2ss-3**SP → **2as-3**SP → **2as-4**SS → **2as-5**SP/PP for dimeric *syn*- and *anti*-butenyl species; **2ss-3**SP + *cis*-BD → **3s**-SS (+ **3s**-SS) → **4s**-SS (+ **3s**-SS) → **5s**-SP/PP (+ **3s**-SS) and **2ss-3**SP + *cis*-BD → **3s**-SS (+ **3s**-SS) → **4s**-SS (+ **3s**-SS) → **4a**-SS (+ **3s**-SS) → **5a**-SP/PP (+ **3s**-SS) for monomeric *syn*- and *anti*-butenyl species, with the isomerization barrier supposed to be low. c) Intrinsic isomerization barriers are defined as the energetic difference between the isomerization transition states and the most stable isomer of the corresponding *anti*-butenyl π complexes (note the *anti* insertion), namely **2aa-3**SP → **2-7a** and **2as-3**SP → **2-7s** for

  0947-6539/01/0717-3694 $ 17.50+.50/0

dimeric species; **3a**-SS → **7** for monomeric species. d) Absolute isomerization barriers are defined as the energetic difference between the isomerization transition states and the overall most stable *anti*-butenyl π complex (note the *anti* insertion), namely **2sa-3**SP → **2-7a** and **2sa-3**SP → **2as-3**SP → **2-7s** for dimeric species; **2sa-3**SP + *cis*-BD → **3a**-SS (+ **3s**-SS) → **7** (+ **3s**-SS) for monomeric species. e) The absolute activation barriers are defined as the energetic difference between the transition states that were passed through along the minimum energy pathway and the most stable π complex; namely, the *anti*-butenyl π complex (note the *anti* insertion) for isomerization (**2sa-3**SP → **2-7s**) and its *syn* counterpart for insertion (**2ss-3**SP → **5a**/**5s**), respectively.

[24] S. Tobisch, R. Taube, *Organometallics* **1999**, *18*, 3045.

[25] a) In this investigation, we have adopted $[C_8H_{13}Ni(C_4H_6)X]$ complexes (with $X^- = Cl^-$, Br^-, I^-) for **7** by extending the butenyl group's model by the next C_4 unit (cf. Figure 5). b) To compare the barriers for isomerization and insertion (following k_{1t}) along the minimum energy pathway in monomeric complexes, species of the same sum formula, namely, $[C_8H_{13}Ni(C_4H_6)X]$ (with $X^- = Cl^-$, Br^-, I^-) were adopted. Therefore, **3s/4s-**SS and **5s-**SP/PP were supplemented by an additional noncoordinating C_4 unit in the best possible arrangement, which has a negligible influence on the energetics.

[26] J. I. Seemann, *Chem. Rev.* **1983**, *83*, 83.

[27] Since the coordination of the first double bond on the growing chain is necessary to form stable **4′** complexes, the calculations were performed on $[C_7H_{11}Ni(C_4H_6)X]$ species (with $X^- = [C_4H_7NiY_2]^-$, $Y^- = Cl^-$, Br^-, I^-). For the **4′** and **5′** species with a weakly coordinating counteranion, entropy contributions cannot be reliably estimated by the theoretical methods employed in this study. Therefore, enthalpies were used to estimate the probability for polymerization to proceed along the k_1 or the k_2 channel, respectively.

[28] a) L. Porri, M. Aglietto, *Macromol. Chem.* **1976**, *177*, 1465; b) L. M. Stephenson, C. A. Kovac, *ACS Symp. Ser.* **1983**, *212*, 307.

Received: December 22, 2000 [F2960]